Dynamic Longitudinal Stability Measurements on a Single-rotor Helicopter (Hoverfly Mk. I)

By
W. STEWART, B.Sc.
with an Appendix on the theoretical estimation of the stability
By
G. J. SISSINGH

COMMUNICATED BY THE PRINCIPAL DIRECTOR OF SCIENTIFIC RESEARCH (AIR), MINISTRY OF SUPPLY

Reports and Memoranda No. 2505
February, 1948*

Summary.—Flight measurements have been made of the phugoid motion of the *Hoverfly* Mk. I helicopter, following an arbitrary longitudinal displacement of the control, the latter being returned to its initial position and held fixed. The tests were done throughout the speed range for power-on conditions and in autorotation for various centre of gravity positions and for forward and backward initial displacement of the stick.

In power-on flight there is a large variation in the dynamic stick-fixed stability with speed. From zero airspeed up to 35 m.p.h. and at airspeeds above 50 m.p.h. the phugoid motion is divergent, but for the speed range 35 to 50 m.p.h. the helicopter is stable.

In autorotation, there is little change in the dynamic stability with speed. Below about 30 m.p.h. the phugoid amplitude tends to increase slowly, and above this speed the amplitude tends to decrease slowly.

There is no variation in the character of the longitudinal phugoid motion with change in centre of gravity position. Neither was any difference detected in the character of the oscillations produced by initial backward movement of the stick, compared with those produced from initial forward displacement.

The theoretical estimation of the power-on stability agrees with the flight tests at low airspeeds, but it shows little variation in stability with speed. In autorotation, the theoretical work agrees very well with the flight tests throughout the speed range. The discrepancy in the power-on tests is felt to be due to a large variation of the fuselage pitching moment with speed, particularly due to the effects of the induced flow from the rotor.

1. *Introduction.*—Flight measurements of dynamic stability were considered one of the more important items of helicopter research work, due to the influence on the flying qualities of the helicopter and to the dearth of full-scale information. The helicopter has now developed from an experimental type of flying machine into an operational and commercial aircraft and the stage has been reached where considerably more attention must be paid to its general flying qualities.

During a series of general handling tests on the *Hoverfly I* helicopter[1] an initial investigation of its longitudinal behaviour was made. These tests were of a qualitative nature and the technique followed closely on the lines adopted on orthodox aircraft. It was shown that the stick-free motion was purely divergent, the stick moving with the divergence, *i.e.*, the stick moved forward as the dive steepened and the speed increased. In normal flight, it is the stick-free behaviour which is most apparent to the pilot, and he must make continuous corrections against the inherent divergent movements of the stick from its trimmed position. As the stick-free motion was purely divergent, no further measurements were made in these conditions.

* R.A.E. Report No. Aero. 2244, received 17th June, 1948.

In the stick-fixed tests[1] the ensuing motion of the helicopter was found to be of a phugoid nature. The difficulty of maintaining the stick fixed in its initial position after a displacement and the possible influence of the sensitive nature of the control on the behaviour of the helicopter were pointed out. Also, as it was not anticipated that there would be any large variation in behaviour with speed, particular attention was not paid to the initial conditions. However, these handling tests did provide valuable information on the technique required in obtaining accurate measurements of the phugoid motion.

An interim note[6] was issued, giving the preliminary results of the dynamic stability measurements in the level flight conditions. The present report covers the complete range of the tests for level flight and autorotational conditions.

The flight measurements were made on a *Hoverfly I*, *i.e.*, Sikorsky R-4B helicopter, during the period July, 1946 to April, 1947.

2. *Description of Helicopter and Instrumentation.*—The helicopter used in these tests was Hoverfly KL109. It has a single three-bladed main rotor of 38-ft diameter and a three-bladed vertical tail rotor. The maximum all-up weight is 2,800 lb. Complete descriptions of the helicopter and of its control system, including photographs, are given in R. & M. 2431[1].

An auto-observer was installed, photographed by a 35-mm Bell and Howell camera, fitted with a solenoid to give remote-controlled single-shot action. Desynn transmitters were fitted to the two rods operating the swash plate controlling the cyclical pitch change of the blades and were calibrated in terms of the stick position and of the cyclical pitch applied to the blades. Desynn receivers connected in parallel with those in the auto-observer were placed in front of the pilot. Desynn transmission was also used for measuring the collective pitch of the main rotor blades and the pitch of the tail rotor blades.

As pointed out in Ref. 2, the aircraft airspeed system does not give accurate speed measurements, due to complex variations in the position error with speed, power, etc.

A special trailing pitot-static system (with an 80-ft line) was used to obtain pitot and static pressures free from the interference from the helicopter. The pitot-static was mounted in a gimbal and ball-race, allowing complete freedom to swivel in any direction. A differential pressure gauge (used as a low-reading airspeed indicator), an altimeter and a rate-of-climb meter were connected to the trailing pitot-static system. A low-reading airspeed indicator was connected in parallel with the auto-observer instruments and placed in front of the pilot. The airspeed measurements were used primarily to give the initial flight conditions, and it will be appreciated that during the phugoid motion the trailing pitot-static indications may lag behind the actual helicopter conditions.

An electrically-driven free gyro was installed to read change in attitude. The gyro could be reset from the observer's position at the beginning of each run.

A normal accelerometer, engine boost gauge, engine and rotor r.p.m. indicators and a timing clock were also incorporated in the auto-observer.

3. *Flight Testing Technique.*—The essential feature of the flight testing technique was to make certain that the control was returned to, and remained steady, in its initial position after displacement. It was not considered advisable nor practical to fit a rigid clamp to the controls, due to the vibration present. During the tests the pilot obtained the steady initial conditions required and noted the desynn reading of the stick position. The control was then displaced, returned to its initial position and firmly held by the pilot. The firmness of the pilot's grip was the main feature in maintaining the trimmed position, and the use of the Desynn indications to ensure that the stick did not wander from its initial position was a secondary consideration. Attempts were made to maintain the constant control position by holding the stick loosely and trying to keep the Desynn readings constant, but this led to continuous over-correction.

Simultaneous time histories of the flight conditions and control positions were obtained during the longitudinal phugoid motion. On analysis of the films the only measurements used were those in which the control position variations during the motion were very small. In the majority of the records the random variations in the stick position during the run were within $\pm\frac{1}{4}$ in. of the trimmed position corresponding to a change in cyclical pitch amplitude of 0·3 deg.

4. *Range of Tests.*—The stick-fixed longitudinal stability tests covered power-on and autorotational conditions throughout the speed range 0 to 60 m.p.h. at various loading conditions.

The power-on phugoid tests were started from straight and level flight at constant height, except at the very low airspeeds, where there was insufficient power to maintain height. There was therefore a power variation with forward speed and the initial conditions of boost pressure, engine and rotor r.p.m. and blade-pitch angle are given graphically in Fig. 1.

In the autorotation tests, the majority of the measurements were made at the minimum pitch of $2\frac{1}{2}$ deg, but a few tests were done at 4 deg pitch. The rotor speed and rate of descent are given against forward airspeed in Fig. 2.

All tests were made at a height of about 3,000 ft.

The power-on measurements were made at four loading conditions and three centre of gravity positions as detailed below, the fourth condition being a check flight at higher weight but at the same centre of gravity position, as in Case 1.

Case	*Take-off Weight*	*C.G. Position*
1	2700	0·5 in. aft of rotor shaft
2	2730	3·0 in. aft of rotor shaft
3	2800	3·0 in. forward of shaft
4	2800	0·5 in. aft of shaft.

In the autorotation tests only loadings 1 and 3 were used.

In each condition measurements of the longitudinal phugoid motion were made for backward and for forward initial displacement of the stick.

5. *Method of Analysis.*—The variations of the helicopter attitude with time, obtained from the attitude gyro records, were used to define the period and damping factor of the phugoid motion, as speeds could not be measured to the required accuracy during the changing conditions, particularly at the lower end of the speed range.

The envelope of the attitude-time oscillations was assumed to be of the form

$$\theta = \theta_0 e^{\lambda t},$$

where θ represents the attitude angle

and λ the damping factor.

In some conditions the phugoid motion was so rapidly divergent that it was not possible to draw the envelope curve. The value of λ in such cases was obtained by using any two peaks of the phugoid θ_1 and θ_2 occurring at times t_1 and t_2 according to the formula

$$\lambda = \frac{\log_e (\theta_2/\theta_1)}{t_2 - t_1}.$$

The possible length of run during the phugoid motion varied considerably with the initial conditions. In the power-on conditions, at about 60 m.p.h. the divergence was rapid, and this necessitated recovery action during the third period of the oscillation. At 50 m.p.h. the phugoid was of constant amplitude and could be continued for any desired length of time.

In most cases five to six consecutive periods were measured, but in one or two runs the motion was continued as far as ten periods. Between 20 and 30 m.p.h. the rate of divergence of the oscillation was so great that, for the smallest practical initial displacement, the speed during the second period became negative with the helicopter in a nose-up attitude. As the 'tail slide' developed there was a serious nose-down pitching of the helicopter. The angular velocity during this, as obtained from the time histories of the attitude, was of the order of 20 deg/sec, but cases of over 40 deg/sec have been measured. Even with recovery action taken on the controls the helicopter had achieved nose-down attitudes of about 60 deg in some cases when the rotation stopped. In some cases the pitching motion was accompanied by a yawing motion of the helicopter.

Below 20 m.p.h. it was impossible to obtain satisfactory phugoids from a backward displacement of the stick, as the nose-up attitude of the helicopter reduced the airspeed below zero and the nose-down pitching motion occurred during the first period. For a forward displacement one complete period could be obtained before the pitching occurred, and this allowed an evaluation of the damping factor.

The pitching motion described above was identical with the behaviour of the helicopter following blade-pitch reduction from high blade angles, when flying at zero airspeed, as discussed in Ref. 1.

In autorotation the dynamic stability is about neutral and does not vary largely with speed. The main limitation to the length of run is the height available for obtaining steady conditions, carrying out the test and regaining level flight. At very low airspeed it is extremely difficult to obtain a simple phugoid, as the longitudinal motion soon develops into a rotary swinging motion like that of a descending parachute.

6. *Results.*—Typical time histories of the airspeed, height, attitude and control positions during the longitudinal phugoid motion are given in Figs. 3 to 9. These records have been selected to illustrate the different stability conditions encountered at the various speeds in power-on and autorotational flight.

The dynamic stability characteristics are given in terms of the damping factor, periodic time of oscillation, and time to double (or halve) the amplitude in Figs. 10, 11 and 12 respectively for the power-on conditions. It will be seen that there are large changes in the stability with speed. At low airspeed the period is about 17 sec and the time to double the amplitude is about 5 sec. At about 35 m.p.h. there is a sudden improvement in stability from a rapidly divergent oscillation to an equally rapidly damped one within a speed range of a few m.p.h. At 40 m.p.h, the period is 14 sec and the time to halve the amplitude about 6 sec. The stability then deteriorates. giving a constant amplitude oscillation with a 17-sec period at 50 m.p.h. and divergent oscillations at higher speeds.

It is worthy of note that at 50 m.p.h. the constant-amplitude oscillation occurred in every case and could be continued for any desired length of time. However, at 35 m.p.h. a constant-amplitude phugoid was obtained in only one case, and it lasted for three periods before a divergent oscillation developed. In all other cases (many of which were not recorded by auto-observer) an increasing or decreasing oscillation was encountered, the increasing oscillation occurring much more frequently.

The stability characteristics in autorotation are given in Figs. 13 and 14 in terms of damping factor and period of oscillation respectively. In this case the times to double or halve the amplitude are very long and have not been given. In autorotation there is little change in the dynamic stability with speed. The period is roughly constant at 13½ sec throughout the speed range, and the amplitude increases slowly for speeds below about 30 m.p.h. and decreases slowly above this speed.

In both the power-on and autorotation tests there is no measurable difference in the longitudinal motion set up from forward or from backward initial displacement of the stick. A difference in

behaviour was quoted in Ref. 1, but as these tests were of a general nature, done at what is now known to be a condition of changing stability with speed and no direct check on the accuracy of the stick position, they should be disregarded in the light of the present tests.

The effect of centre of gravity variation was tested mainly in the power-on conditions and no difference in the longitudinal behaviour of the helicopter could be detected as the centre of gravity position was varied.

7. *Comparison with Theoretical Estimation.*—A theoretical estimation of the dynamic stability characteristics, for comparison with the flight measurements, has been made by G. J. Sissingh. In Appendix I an outline of the theoretical treatment is given. A general single-rotor configuration with hinged blades is discussed and then the particular Sikorsky R-4B layout is considered under the given test conditions. Indications of the methods of obtaining the various rotor derivatives are also given. The available wind-tunnel data for the rotor and fuselage derivatives was very poor, but the assumptions made in the use of these derivatives are also included in the Appendix.

The comparison of the theoretical estimation with the flight measurements is included in Figs. 10 and 11 for the power-on conditions and in Figs. 13 and 14 for the autorotation tests. It will be seen that in the level flight conditions the comparison is very good at low airspeed. At about 35 m.p.h. the measured stability improves very rapidly but this is not shown by the theoretical estimation. This discrepancy is thought to be due to the influence of the fuselage pitching moment. In hovering or at very low airspeed the slipstream is roughly uniform and acts downwards on areas of the same order fore and aft of the lateral axis through the centre of gravity. As the airspeed increases the slipstream is inclined backward and affects only the fuselage aft of the centre of gravity. As the airspeed is further increased the slipstream affects less and less of the fuselage surfaces, and also the velocity of the air in the slipstream approaches that of the free air. Thus, changes in fuselage pitching moment with forward speed and with power would be expected in the static condition. In addition there will be changes in pitching moment with attitude. The linear and angular accelerations during the oscillatory motion will introduce further effects from the fuselage pitching moment. The effect of the induced flow from the rotor on the fuselage pitching moment could not be allowed for in the theoretical treatment.

In the autorotation tests the comparison of the estimated and measured quantities is very good throughout the speed range. A better agreement in autorotational flight than in power-on conditions was to be expected due to the lack of induced flow effects and to the fact that there are more available wind-tunnel data on rotor characteristics for low values of blade pitch.

8. *Effect of Gusts.*—It was particularly noticeable in flying the helicopter that atmospheric gusts had very much less effect than that usually experienced on fixed-wing aircraft. This feature, commented on briefly in the report on the general handling tests[1], was confirmed in the present series of tests.

Several flights were made in rough air conditions at 20 and 60 m.p.h. in level flight, *i.e.*, in the regions of instability. As previously there were small variations in the stick position, as a rigid clamp was not used. These variations were slightly greater than in the phugoid tests, due to the effect of the helicopter motion in the rough air, particularly directionally, on the pilot's attempts to keep the stick fixed. The effect of these stick displacements may be relatively important. However, with this experimental limitation on the accuracy of the stick-fixed position, the helicopter was flown through severe gusts without showing any tendency to develop the unstable phugoids.

A preliminary theoretical investigation of the effect of gusts on the helicopter shows this to be of an entirely different nature to that produced from stick displacement. Whereas a fore-and-aft movement of the stick produces a longitudinal tilting of the disc, flying straight into a gust gives a direct effect on the lift and a lateral tilting of the disc. This is, of course, due to the phase difference between the change in incidence of a hinged blade and the position of resultant blade

displacement. There is also a tendency to produce a longitudinal tilting of the disc, but as this term is only of the order of one-tenth of the lateral moment and the pitching moment of inertia of the helicopter is about ten times that in roll, the longitudinal effect is negligible in comparison to the lateral effects. Thus, stated simply, the effect of flying a helicopter with flapping blades straight into a vertical gust produces a roll of the helicopter.

9. *Conclusions.*—9.1. In level flight with the stick fixed the longitudinal phugoid motion of the Hoverfly I is very unstable at low airspeeds. At about 35 m.p.h. the stability suddenly improves, and there is a stable region from 35 to 50 m.p.h. Above 50 m.p.h. the helicopter is again unstable.

9.2. The rapid changes in stability with speed in the power-on conditions are thought to be due to the influence on the induced flow from the rotor on the fuselage pitching moments.

9.3. In autorotation the helicopter is slightly unstable below 30 m.p.h. and becomes stable above this speed.

9.4. The position of the centre of gravity has no effect on the stick-fixed longitudinal stability.

9.5. No difference could be detected between oscillations produced by initial forward movement of the stick compared with those produced from initial backward movement.

9.6. The theoretical estimation of the stability agrees with the flight tests in autorotation and at low airspeeds in the power-on conditions. At higher forward speeds there is a large discrepancy, where the rapid changes of stability with speed were found in flight.

10. *Further Developments.*—10.1. Further stability tests will be made on another type of helicopter (the Sikorsky S-51) where absence of vibration in the stick will improve the flight test accuracy and the fuselage will have a much smaller influence on the behaviour of the helicopter.

10.2. The influence of a tailplane on the stability of the helicopter will also be investigated.

10.3. A more detailed investigation of the effect of gusts on the helicopter in theory and by flight tests will be made.

10.4. A general report on the theoretical estimation of the stability of the single-rotor helicopter with hinged blades is in preparation.

LIST OF SYMBOLS

A		Non-dimensional coefficient of rotor
a		Slope of lift curve of blade section
a_0	radn	Coning angle
a_1	radn	Coefficient of $\cos\psi$ in Fourier series for flapping angle
$a_{1,u}$		$= \partial a_1/\partial u$
$a_{1,w}$		$= \partial a_1/\partial w$
$a_{1,q}$		$= \partial a_1/\partial q$
$a_{1,\mu 1}$		$= \partial a_1/\partial \mu_1$
$a_{1,\alpha}$		$= \partial a_1/\partial \alpha$
B		Factor allowing for tip loss, generally taken as 0·98

b		Number of blades of rotor
b_1	radn	Coefficient of sin ψ in Fourier series for flapping angle
c	ft	Chord of blade at $0{\cdot}7R$
C_L, C_D		Lift, drag coefficients of rotor referred to flight speed and disc area
		$C_L = \dfrac{L}{\frac{1}{2}\rho V^2 \pi R^2} = \dfrac{k_L}{\mu_1^2}$ $\qquad$ $C_D = \dfrac{D}{\frac{1}{2}\rho V^2 \pi R^2} = \dfrac{k_D}{\mu_1^2}$
$C_{D,f}$		Fuselage drag coefficient, $= \dfrac{D_f}{\frac{1}{2}\rho V^2 \pi R^2}$
$C_{m,f}$		Fuselage pitching-moment coefficient, $= \dfrac{M_f}{\frac{1}{2}\rho V^2 \pi R^2 . R}$
$C_{L,a}$		$\partial C_L / \partial \alpha$
$C_{L,\mu 1}$		$\partial C_L / \partial \mu_1$
$C_{D,a}$		$\partial C_D / \partial \alpha$
$C_{D,\mu 1}$		$\partial C_D / \partial \mu_1$
$C_{D,fi}$		$\partial C_{D,f} / \partial i$
D	lb	Rotor drag
D_f	lb	Fuselage drag
eR	ft	Distance of flapping hinge from axis of rotation
fR	ft	Fore-and-aft position of rotor shaft relative to c.g. of helicopter
f_1		$f \cos i - h \sin i$
f		Suffix denoting fuselage
hR	ft	Distance of rotor hub above c.g.
h_1		$h \cos i + f \sin i$
I	ft lb sec^2	Total moment of inertia of helicopter about y-axis
I_b	ft lb sec^2	Contribution of the blades to I where
		$I_b = \dfrac{bW_b(hR)^2}{g}\left[1 + \dfrac{f^2}{h^2} + \dfrac{a_0 S}{h} + \dfrac{e(e+s)}{2h^2}\right]$
I_1	ft lb sec^2	Moment of inertia of blade about flapping hinge
i	radn	Rotor incidence, angle between relative wind and a plane perpendicular to the rotor shaft
k_L, k_D		Lift, drag coefficients of rotor referred to tip speed and disc area
		$k_L = \dfrac{L}{\frac{1}{2}\rho(\Omega R)^2 \pi R^2}$ $\qquad$ $k_L = \dfrac{D}{\frac{1}{2}\rho(\Omega R)^2 \pi R^2}$
k_T		Thrust coefficient $k_T = \dfrac{T}{\frac{1}{2}\rho(\Omega R)^2 \pi R^2}$
$k_{L,a}$		$\partial k_L / \partial \alpha$
$k_{L,\mu 1}$		$\partial k_L / \partial \mu_1$
$k_{D,a}$		$\partial k_D / \partial \alpha$
$k_{D,\mu 1}$		$\partial k_D / \partial \mu_1$

L	lb	Rotor lift
M	lb ft	Pitching moment
M_1	lb ft	Weight moment of blade about flapping hinge
M_u		$\partial M/\partial u$
M_w		$\partial M/\partial w$
M_q		$\partial M/\partial q$
q	radn/sec	Angular velocity of helicopter about the y-axis
q_0	radn/sec	Angular velocity of helicopter about the rotor hub centre
r		Root of the frequency equation
r		Suffix denoting rotor
R	ft	Rotor radius
πR^2	ft^2	Rotor disc area
sR	ft	Distance of c.g. of blade from flapping hinge
S	lb	Centrifugal force of all blades
T	lb	Thrust of rotor in hovering flight
T_0	sec	Periodic time of oscillation
T_H	sec	Time to half amplitude in a damped oscillation
T_D	sec	Time to double amplitude in an increasing oscillation
u	ft/sec	Small disturbance of velocity V in the x-direction
V	ft/sec	Velocity of undisturbed flight
w	ft/sec	Small disturbance of velocity V in the z-direction
W	lb	Weight of helicopter
W_b	lb	Weight of one rotor blade
x, y, z		Rectangular system of axes with origin coincident with c.g. of helicopter and the x-axis indicates direction of undisturbed flight
X, Y, Z	lb	Forces in direction of corresponding axes
X_u, X_w, X_q		$\partial X/\partial u$, $\partial X/\partial w$, $\partial X/\partial q$
Z_u, Z_w, Z_q		$\partial Z/\partial u$, $\partial Z/\partial w$, $\partial Z/\partial q$
α	radn	Effective angle of attack of rotor $= i + \vartheta_s$
β	radn	Flapping angle $\beta = a_0 - a_1 \cos \Psi - b_1 \sin \Psi - \ldots\ldots$
γ_0		Mass constant of blade $= \dfrac{R^4 \rho c a}{I_1}$
γ		Apparent mass constant of blade
η		Non-dimensional aerodynamic coefficient of rotor
θ	radn	Angle of rotation in pitch
θ_1, θ_2		Angles of rotation in pitch at times t_1 and t_2
ϑ	radn	Instantaneous pitch of blade at 0·7 radn and given by $\vartheta = \vartheta_0 + \vartheta_s \sin \psi$

ϑ_0	radn	Pitch of blade with no cyclical pitch imposed
ϑ_s	radn	Cyclical pitch due to longitudinal control
λ		Damping coefficient for the longitudinal motion
μ_1		Tip speed ratio $V/\Omega R$
$\mu_{1,\alpha}$		$\partial\mu_1/\partial\alpha$
ν		Non-dimensional aerodynamic coefficient of rotor
ρ	slugs/ft^3	Air density
σ		Solidity of rotor $= bc/\pi R$
τ	radn	Angle of climb
χ	radn	Attitude of rotor shaft relative to the vertical positive if the shaft is inclined backward
ψ	radn	Blade azimuth angle measured from downwind position in the direction of rotation
Ω	radn/sec	Angular velocity of rotor
ΩR	ft/sec	Tip speed of rotor

REFERENCES

No.	*Author*	*Title, etc.*
1	W. Stewart	General Handling Tests of the Sikorsky R-4B Helicopter (*Hoverfly* Mk. I). R. & M. 2431. October, 1946.
2	W. Stewart	Brief Performance Tests on the *Hoverfly* Mk. 1 by the Aneroid Method and by Flight Path Recorder. A.R.C. 10,733. May, 1947.
3	Sissingh and Nagel	Survey of German Research and Development in the Field of Rotary Wing Aircraft. Monograph N, AVA. 1946.
4	K. Hohenemser	Longitudinal Stability of the Helicopter in Straight Symmetrical Flight. F.B. 1989/2. 1944.
5	J. B. Wheatley and C. Bioletti ..	Wind Tunnel Tests of 10-ft Diameter Autogyro Rotors. A.R.C. 2533. (Unpublished.)
6	W. Stewart	Interim Note on the Dynamic Longitudinal Stability of a Single-rotor Helicopter (*Hoverfly* I). A.R.C. 10,646. April, 1947.

APPENDIX I

Calculation of the Longitudinal Dynamic Stability

1. *Equations of Motion.*—The equations of motion are referred to the normal rectangular x, y, z-system of axes, with the origin coincident with the centre of gravity of the helicopter and the x-direction parallel to the flight path.

The equations for the equilibrium of the forces and moments (*see* Fig. 15) may be written

$$X_u u + X_w w + X_q q - W\theta \cos\tau - \frac{W}{g}\dot{u} = 0\,, \quad .. \quad .. \quad .. \quad (1)$$

$$Z_u u + Z_w w + Z_q q - W\theta \sin\tau + \frac{W}{g} Vq - \frac{W}{g}\dot{w} = 0\,, \quad .. \quad .. \quad .. \quad (2)$$

$$M_u u + M_w w + M_q q - I\dot{q} = 0\,. \quad .. \quad .. \quad .. \quad (3)$$

These equations could be conveniently expressed in non-dimensional form by taking the mass of the helicopter (W/g) as the unit of mass, the rotor radius (R) as the unit of length and $W/g\rho V\pi R^2$ or $W/g\rho\,\Omega R\pi R^2$ as the unit of time, the latter unit of time being used when hovering conditions are being considered.

The pitching moment about the centre of gravity due to the rotor (*see* Fig. 16) is given as

$$M_r = -RX_r\,(h\cos i + f\sin i) - RZ_r\,(f\cos i - h\sin i) + \tfrac{1}{2}SeRa_1\,, \quad (4)$$

where the last term is introduced by the flapping motion of the blades.

Substituting, $h_1 = h\cos i + f\sin i$ .. .. (5)

and $f_1 = f\cos i - h\sin i$, ... (6)

equation (4) gives

$$M_{r,u} = R\left(\frac{Se}{2\Omega R}a_{1,\mu 1} - X_{ru}h_1 - Z_{ru}f_1\right), \quad .. \quad .. \quad .. \quad .. \quad .. \quad (7)$$

$$M_{r,w} = R\left(\frac{Se}{2V}a_{1,\alpha} - X_{rw}h_1 - Z_{rw}f_1\right), \quad .. \quad .. \quad .. \quad .. \quad .. \quad (8)$$

$$M_{r,q} = R\left(\frac{Se}{2}a_{1,q} - X_{rq}h_1 - Z_{rq}f_1\right), \quad .. \quad .. \quad .. \quad .. \quad .. \quad .. \quad (9)$$

where $a_{1,\mu 1}$, $a_{1,\alpha}$ and $a_{1,q}$ denote the differentials of a_1 with respect to μ_1, α and q respectively.

The rotation of the helicopter about its centre of gravity imposes on the hub linear velocities

$-h_1R_q$ in the *x-direction*

and $-f_1R_q$ in the *z-direction*.

Hence, we may write

$$X_{r,q} = X_{r,q0} - h_1RX_{r,u} - f_1RX_{r,w}\,, \quad .. \quad .. \quad .. \quad .. \quad .. \quad .. \quad (10)$$

$$Z_{r,q} = Z_{r,q0} - h_1RZ_{r,u} - f_1RZ_{r,w}\,, \quad .. \quad .. \quad .. \quad .. \quad .. \quad .. \quad (11)$$

$$a_{1,q} = a_{1,q} - \frac{h_1}{\Omega}a_{1,\mu 1} - \frac{f_1}{\Omega\mu_1}a_{1,\mu}\,. \quad .. \quad .. \quad .. \quad .. \quad .. \quad .. \quad (12)$$

In these equations $X_{r,q0}$, $Z_{r,q0}$ and $a_{1,q0}$ represent rates of change with respect to the angular velocity q_0 about the rotor hub centre.

The derivatives $X_{r,u}$, $X_{r,w}$, $Z_{r,u}$, $Z_{r,w}$, $a_{1,\alpha}$ and $a_{1,\mu 1}$ are generally obtained from wind-tunnel data, *i.e.*, from curves of lift, drag and a_1 against speed ratio and 'effective' rotor incidence α, where the latter is given by

$$\alpha = i + \vartheta_s \,, \quad \ldots \quad \ldots \quad \ldots \quad \ldots \quad \ldots \quad \ldots \quad \ldots \quad \ldots \quad \ldots \quad (13)$$

$$= \chi - \tau + \vartheta_s \,. \quad \ldots \quad \ldots \quad \ldots \quad \ldots \quad \ldots \quad \ldots \quad \ldots \quad \ldots \quad (14)$$

There are no available measurements of the rotary derivatives, and these must therefore be estimated from the following equations.

$$a_{1,q0} = -\frac{16}{\gamma\Omega(B^4 - \frac{1}{2}B^2\cos^2 i)} \,, \quad \ldots \quad \ldots \quad \ldots \quad \ldots \quad \ldots \quad \ldots \quad (15)$$

$$X_{r,q0} = -\eta T a_{1,q0} = \frac{16\eta W}{\gamma\Omega(B^4 - \frac{1}{2}B^2\cos^2 i)} \,, \quad \ldots \quad \ldots \quad \ldots \quad \ldots \quad \ldots \quad (16)$$

$$Z_{r,q0} = 0 \,. \quad \ldots \quad \ldots \quad \ldots \quad \ldots \quad \ldots \quad \ldots \quad \ldots \quad \ldots \quad \ldots \quad (17)$$

The coefficient γ represents the apparent mass constant of the blades, and due to the unequal distribution of the downwash during the pitching motion, especially at low tip speed ratios, this value is considerably smaller than the true value of γ_0. The coefficients η and γ/γ_0 can be taken from the graphs in Figs. 21 to 22 for hovering flight. Both factors increase with increase in tip-speed ratio and approach the value unity.

2. *Hovering Flight.*—Hovering flight may be interpreted as a level flight condition with velocity $V = 0$ and the x-axis in the undisturbed state horizontal, *i.e.*, $\tau = 0$. These conditions are shown diagrammatically in Fig. 17. As the influence of the fuselage derivatives may be neglected and the rotor derivatives $X_{r,w}$, $Z_{r,q}$ and $M_{r,w}$ are zero, the equations of motion (1), (2), (3) become

$$X_{r,u}u + X_{r,q}q - W\theta - \frac{W}{g}\dot{u} = 0 \,, \quad \ldots \quad \ldots \quad \ldots \quad \ldots \quad \ldots \quad \ldots \quad (18)$$

$$Z_{r,w}w - \frac{W}{g}\dot{w} = 0 \,, \quad \ldots \quad \ldots \quad \ldots \quad \ldots \quad \ldots \quad \ldots \quad \ldots \quad \ldots \quad (19)$$

$$M_{r,u}u + M_{r,q}q - I\dot{q} = 0 \,. \quad \ldots \quad \ldots \quad \ldots \quad \ldots \quad \ldots \quad \ldots \quad \ldots \quad \ldots \quad (20)$$

From equation (19) it will be seen that the vertical motion of the helicopter is aperiodic. The exponential index (r) is $gZ_{r,w}/W$, and as $Z_{r,w}$ is always negative this disturbance is damped. Equations (18) and (20) give the frequency equation

$$r^3\frac{WI}{g} - r^2\left(\frac{M_{r,q}W}{g} + IX_{r,u}\right) + r(X_{r,u}M_{r,q} - X_{r,q}M_{r,u}) + WM_{r,u} = 0 \,. \quad \ldots \quad (21)$$

For the Sikorsky configuration the centre of gravity is on the rotor shaft and the flapping hinges have no offset, *i.e.*,

$$e = f = 0. \quad \ldots \quad \ldots \quad \ldots \quad \ldots \quad \ldots \quad \ldots \quad \ldots \quad \ldots \quad \ldots \quad \ldots \quad (22)$$

Hence,

$$M_{r,q} = -hRX_{r,q} \,, \quad \ldots \quad \ldots \quad \ldots \quad \ldots \quad \ldots \quad \ldots \quad \ldots \quad \ldots \quad \ldots \quad (23)$$

$$M_{r,u} = -hRX_{r,u} \,. \quad \ldots \quad \ldots \quad \ldots \quad \ldots \quad \ldots \quad \ldots \quad \ldots \quad \ldots \quad \ldots \quad (24)$$

Thus the term r in equation (21) vanishes, and by Routh's criterion hovering flight instability with this configuration is unavoidable.

If no wind-tunnel data is available the necessary rotor derivatives may be calculated from the following equations.

$$X_{r,u} = \frac{W}{\Omega R} A \,, \quad \ldots \quad \ldots \quad \ldots \quad \ldots \quad \ldots \quad \ldots \quad \ldots \quad \ldots \quad \ldots \quad (25)$$

$$X_{r,w} = 0 \,, \quad \ldots \quad \ldots \quad \ldots \quad \ldots \quad \ldots \quad \ldots \quad \ldots \quad \ldots \quad \ldots \quad (26)$$

$$X_{r,q0} = \frac{16\eta W}{\gamma \Omega B^4} \,, \quad \ldots \quad \ldots \quad \ldots \quad \ldots \quad \ldots \quad \ldots \quad \ldots \quad \ldots \quad \ldots \quad (27)$$

$$X_{r,q} = \frac{W}{\Omega}\left(\frac{16\eta}{\gamma B^4} + Ah\right), \quad \ldots \quad \ldots \quad \ldots \quad \ldots \quad \ldots \quad \ldots \quad \ldots \quad (28)$$

$$Z_{r,u} = 0, \quad \ldots \quad \ldots \quad \ldots \quad \ldots \quad \ldots \quad \ldots \quad \ldots \quad \ldots \quad \ldots \quad (29)$$

$$Z_{r,w} = -\frac{W}{\Omega R}\frac{2}{(2-\eta)\sqrt{k_T}} \,, \quad \ldots \quad \ldots \quad \ldots \quad \ldots \quad \ldots \quad \ldots \quad \ldots \quad (30)$$

$$Z_{r,q0} = 0 \,, \quad \ldots \quad \ldots \quad \ldots \quad \ldots \quad \ldots \quad \ldots \quad \ldots \quad \ldots \quad \ldots \quad (31)$$

$$Z_{r,q} = \frac{W}{\Omega R}\frac{2f}{(2-\eta)\sqrt{k_T}} \,. \quad \ldots \quad \ldots \quad \ldots \quad \ldots \quad \ldots \quad \ldots \quad \ldots \quad (32)$$

Also, from (7), (8) and (9)

$$M_{r,u} = \frac{Se}{2\Omega} a_{1,\mu 1} - X_{r,u} hR - Z_{r,u} fR \,, \quad \ldots \quad \ldots \quad \ldots \quad \ldots \quad \ldots \quad (33)$$

$$M_{r,w} = \frac{SeR}{2} a_{1,a} - X_{r,w} hR - Z_{r,w} fR \,, \quad \ldots \quad \ldots \quad \ldots \quad \ldots \quad \ldots \quad (34)$$

$$M_{r,q} = \frac{SeR}{2} a_{1,q} - X_{r,q} hR - Z_{r,q} fR \,, \quad \ldots \quad \ldots \quad \ldots \quad \ldots \quad \ldots \quad (35)$$

and the derivatives are given by

$$a_{1,u} = \frac{\nu}{\Omega R} \,, \quad \ldots \quad \ldots \quad \ldots \quad \ldots \quad \ldots \quad \ldots \quad \ldots \quad \ldots \quad \ldots \quad (36)$$

$$a_{1,w} = 0, \quad \ldots \quad \ldots \quad \ldots \quad \ldots \quad \ldots \quad \ldots \quad \ldots \quad \ldots \quad \ldots \quad (37)$$

$$a_{1,q0} = -\frac{16}{\gamma \Omega B^4} \,, \quad \ldots \quad \ldots \quad \ldots \quad \ldots \quad \ldots \quad \ldots \quad \ldots \quad \ldots \quad (38)$$

$$a_{1,q} = -\frac{1}{\Omega}\left(\frac{16}{\gamma B^4} + h\nu\right). \quad \ldots \quad \ldots \quad \ldots \quad \ldots \quad \ldots \quad \ldots \quad \ldots \quad (39)$$

In the above equations, terms containing f can generally be neglected. The coefficients γ, A, ν and the ratio γ/γ_0 can be taken from Figs. 19 to 22. These curves have been calculated for rectangular untwisted blades, but they can also be applied to other shapes of blade if the pitch angle and solidity are referred to the 0·7 radius position.

3. *Helicopter Forward Flight.*—The lift and drag coefficients of the helicopter rotor depend on the incidence α and the tip-speed ratio μ_1. The coefficients C_L and C_D are referred to the disc area and forward velocity, while k_L and k_D are referred to disc area and tip speed.

For equilibrium,

$$k_L = \frac{W \cos \tau}{\frac{1}{2}\rho(\Omega R)^2 \pi R^2} \,, \quad \ldots \quad \ldots \quad \ldots \quad \ldots \quad \ldots \quad \ldots \quad \ldots \quad \ldots \quad (40)$$

$$k_D = -\left(C_{D,f}\mu_1^2 + \frac{W \sin \tau}{\frac{1}{2}\rho(\Omega R)^2 \pi R^2}\right). \quad \ldots \quad \ldots \quad \ldots \quad \ldots \quad \ldots \quad (41)$$

In level flight, $\tau = 0$ and the equations (40), (41) become

$$k_L = \frac{W}{\frac{1}{2}\rho(\Omega R)^2 \pi R^2}, \quad \ldots \quad (42)$$

$$k_D = -C_{D,f}\mu_1^2. \quad \ldots \quad (43)$$

Assuming that the rotor speed is not influenced by the small disturbances, the changes in incidence and tip speed ratio are given by

$$\Delta\alpha = \frac{w}{V}, \quad \ldots \quad (44)$$

$$\Delta\mu_1 = \frac{u}{\Omega R}. \quad \ldots \quad (45)$$

Hence,

$$\Delta_L = \tfrac{1}{2}\rho(\Omega R)^2 \pi R^2 \left(k_{L,\alpha}\frac{w}{V} + k_{L,\mu 1}\frac{u}{\Omega R}\right), \quad \ldots \quad (46)$$

$$\Delta_D = \tfrac{1}{2}\rho(\Omega R)^2 \pi R^2 \left(k_{D,\alpha}\frac{w}{V} + k_{D,\mu 1}\frac{u}{\Omega R}\right). \quad \ldots \quad (47)$$

Thus, the rotor forces may be written

$$\Delta X_r = L\Delta\alpha - \Delta D, \quad \ldots \quad (48)$$

$$\Delta Z_r = -(\Delta L + D\Delta\alpha), \quad \ldots \quad (49)$$

and from (46) and (47)

$$\Delta X_r = \tfrac{1}{2}\rho(\Omega R)^2 \pi R^2 \left(k_L\frac{w}{V} - k_{D,\alpha}\frac{w}{V} - k_{D,\mu 1}\frac{u}{\Omega R}\right), \quad \ldots \quad (50)$$

$$\Delta Z_r = -\tfrac{1}{2}\rho(\Omega R)^2 \pi R^2 \left(k_{L,\alpha}\frac{w}{V} + k_{L,\mu 1}\frac{u}{\Omega R} + k_D\frac{w}{V}\right). \quad \ldots \quad (51)$$

Hence, we obtain the force derivatives

$$X_{r,u} = -\tfrac{1}{2}\rho(\Omega R)\pi R^2 k_{D,\mu 1}, \quad \ldots \quad (52)$$

$$X_{r,w} = \tfrac{1}{2}\rho(\Omega R)\pi R^2 \frac{1}{\mu_1}(k_L - k_{D,\alpha}), \quad \ldots \quad (53)$$

$$Z_{r,u} = -\tfrac{1}{2}\rho(\Omega R)\pi R^2 k_{L,\mu 1}, \quad \ldots \quad (54)$$

$$Z_{r,w} = -\tfrac{1}{2}\rho(\Omega R)\pi R^2 \frac{1}{\mu_1}(k_D + k_{L,\alpha}). \quad \ldots \quad (55)$$

The values of $k_{L,\alpha}$, $k_{L,\mu 1}$, $k_{D,\alpha}$ and $k_{D,\mu 1}$ are generally obtained from wind-tunnel tests. If measurements of the drag derivatives are not available, approximate values can be deduced in terms of the lift and flapping angle.

$$D = L(\alpha + a_1), \quad \ldots \quad (56)$$

$$\Delta D = \frac{D}{L}\Delta L + L(\Delta\alpha + \Delta a_1). \quad \ldots \quad (57)$$

Also,

$$\Delta a_1 = a_{1,\mu 1}\frac{u}{\Omega R} + a_{1,\alpha}\frac{w}{V}. \quad \ldots \quad (58)$$

Hence,

$$\Delta D = \tfrac{1}{2}\rho(\Omega R)^2 \pi R^2 \left[\Delta\alpha\left(\frac{k_D}{k_L} k_{L,\alpha} + k_L + a_{1,\alpha}k_L\right) + \Delta\mu_1\left(\frac{k_D}{k_L} k_{L,\mu 1} + k_L a_{1,\mu 1}\right)\right]. \quad (59)$$

Equations (52) and (53) may be replaced by

$$X_{r,u} = -\tfrac{1}{2}\rho(\Omega R)\pi R^2\left(k_L a_{1,\mu 1} + \frac{k_D}{k_L} k_{L,\mu 1}\right), \quad (60)$$

$$X_{r,w} = -\tfrac{1}{2}\rho(\Omega R)\pi R^2 \frac{1}{\mu_1}\left(k_L a_{1,\alpha} + \frac{k_D}{k_L} k_{L,\alpha}\right). \quad (61)$$

The numerical values for the derivatives $a_{1,\alpha}$ and $a_{1,\mu 1}$ have to be taken from wind-tunnel tests for the effective angle of attack and given by equation (13) or (14).

If the lift and drag coefficients of the rotor are referred to the forward speed, equations (52), (53), (54), (55), (60) and (61) take the form

$$X_{r,u} = -\tfrac{1}{2}\rho V\pi R^2 (2C_D + \mu_1 C_{D,\mu 1}), \quad (52a)$$

$$X_{r,w} = +\tfrac{1}{2}\rho V\pi R^2 (C_L - C_{D,\alpha}), \quad (53a)$$

$$Z_{r,u} = -\tfrac{1}{2}\rho V\pi R^2 (2C_L + \mu_1 C_{L,\mu 1}), \quad (54a)$$

$$Z_{r,w} = -\tfrac{1}{2}\rho V\pi R^2 (C_D + C_{L,\alpha}), \quad (55a)$$

$$X_{r,u} = -\tfrac{1}{2}\rho V\pi R^2\left(2C_D + \mu_1 \frac{C_D}{C_L} C_{L,\mu 1} + \mu_1 C_L a_{1,\mu 1}\right), \quad (60a)$$

$$X_{r,w} = -\tfrac{1}{2}\rho V\pi R^2\left(C_L a_{1,\alpha} + \frac{C_D}{C_L} C_{L,\alpha}\right). \quad (61a)$$

Considering the influence of the fuselage and denoting the drag and pitching-moment coefficients by

$$C_{D,f} = \frac{D_f}{\tfrac{1}{2}\rho V^2\pi R^2}, \quad (62)$$

$$C_{m,f} = \frac{M_f}{\tfrac{1}{2}\rho V^2\pi R^2 . R}, \quad (63)$$

the fuselage derivatives may be written

$$X_{f,u} = -2C_{D,f}\tfrac{1}{2}\rho V\pi R^2, \quad (64)$$

$$X_{f,w} = -C_{D,fi}\tfrac{1}{2}\rho V\pi R^2, \quad (65)$$

$$Z_{f,u} = 0, \quad (66)$$

$$Z_{f,w} = -C_{D,f}\tfrac{1}{2}\rho V\pi R^2, \quad (67)$$

$$M_{f,u} = 2C_{m,f}\tfrac{1}{2}\rho V\pi R^2 . R, \quad (68)$$

$$M_{f,w} = C_{m,fi}\tfrac{1}{2}\rho V\pi R^2 . R. \quad (69)$$

4. *Autorotation.*—In autorotational flight, the incidence and tip-speed ratio of the rotor are no longer independent of each other. For each incidence there is a certain tip-speed ratio, and the rotational speed of the rotor must be considered as an additional degree of freedom. However, it is very difficult to deal with the changes of rotor rotational speed with incidence during the motion, and it is assumed that at each instant the rotational speed corresponds to that in the steady state for the given incidence, as obtained from the relationship in Fig. 2. The variation of rotational speed of the blade during its azimuth travel is also neglected.

In steady flight

$$C_L = \frac{W \cos \tau}{\frac{1}{2}\rho V^2 \pi R^2}, \quad \ldots \quad (70)$$

$$C_D = -\left(C_{D,f} + \frac{W \sin \tau}{\frac{1}{2}\rho V^2 \pi R^2}\right). \quad \ldots \quad (71)$$

Hence, the force derivatives of the rotor are given by

$$X_{r,u} = -\tfrac{1}{2}\rho V \pi R^2 \, 2C_D, \quad \ldots \quad (72)$$

$$X_{r,w} = +\tfrac{1}{2}\rho V \pi R^2 \, (C_L - C_{D,\alpha}), \quad \ldots \quad (73)$$

$$Z_{r,u} = -\tfrac{1}{2}\rho V \pi R^2 \, 2C_L, \quad \ldots \quad (74)$$

$$Z_{r,w} = -\tfrac{1}{2}\rho V \pi R^2 \, (C_D + C_{L,\alpha}). \quad \ldots \quad (75)$$

The numerical values of $C_{L,\alpha}$ and $C_{D,\alpha}$ are generally obtained from wind-tunnel tests. If the curves of C_L and C_D are plotted against tip-speed ratio, it is convenient to write (73) and (75) in the form

$$X_{r,w} = +\tfrac{1}{2}\rho V \pi R^2 \, (C_L - C_{D,\mu 1}\mu_{1,\alpha}), \quad \ldots \quad (76)$$

$$Z_{r,w} = -\tfrac{1}{2}\rho V \pi R^2 \, (C_D + C_{L,\mu 1}\mu_{1,\alpha}), \quad \ldots \quad (77)$$

where the values of $\mu_{1,\alpha}$ is also taken from the tests.

If the drag has to be estimated from the lift and flapping motion, equation (73) is replaced by

$$X_{r,w} = -\tfrac{1}{2}\rho V \pi R^2 \left(\frac{C_D}{C_L} C_{L,\alpha} + C_L a_{1,\alpha}\right), \quad \ldots \quad (78)$$

or

$$X_{r,w} = -\tfrac{1}{2}\rho V \pi R^2 \left(\frac{C_D}{C_L} C_{L,\mu 1}\mu_{1,\alpha} + C_L a_{1,\mu 1}\mu_{1,\alpha}\right). \quad \ldots \quad (79)$$

The other derivatives can be calculated by equations (7) to (12). It is noteworthy that in autorotational flight the derivative M_u is always zero.

5. *Vertical Descent in Autorotation.*—In vertical descent (Fig. 18)

$$\tau = -90 \text{ deg}, \quad C_L = 0, \quad C_D \simeq \frac{W}{\frac{1}{2}\rho V^2 \pi R^2}.$$

Also, if the rotor shaft is vertical and no cyclical pitch is imposed on the blades

$$\chi = 0 \quad \text{and} \quad \alpha = 90 \text{ deg},$$

and due to symmetry

$$C_{D,\alpha} = 0.$$

Neglecting the force derivative of the fuselage we have

$$X_w = Z_u = 0, \quad \ldots \quad (80)$$

and the equations of motion become

$$X_u u - \frac{W}{g}\dot{u} = 0, \quad \ldots \quad (81)$$

$$Z_w w + Z_q q + W\theta + \frac{W}{g} V q - \frac{W}{g}\dot{w} = 0, \quad \ldots \quad (82)$$

$$M_w w + M_q q - I\dot{q} = 0. \quad \ldots \quad (83)$$

As in the hovering state, the vertical motion is no longer coupled with the longitudinal and pitching motions of the helicopter. The vertical motion dies out aperiodically and the exponential index is given by $X_u g/W$.

The other two equations give the frequency equation

$$r^3 \frac{WI}{g} - r^2\left(Z_w I + \frac{W}{g} M_q\right) + r\left(Z_w M_q - M_w Z_q - M_w \frac{W}{g} V\right) - M_w W = 0 , \quad .. \quad (84)$$

where for the Sikorsky R-4B configuration the term $(Z_w M_q - M_w Z_q)$ becomes zero.

The equations for the calculation of the other derivatives are as given before. In determining $Z_{r,w}$ from (75), it should be noted that $C_{L,a}$ is negative, as the lift coefficient decreases with increasing angle of attack.

6. *Numerical Evaluation.*—Due to the lack of appropriate wind-tunnel tests the rotor derivatives in forward flight, both for power-on conditions and in autorotation, were deduced from wind-tunnel tests of intermeshing rotors.[4] The investigation of the vertical descent in autorotation is based on model tests of autogyro rotors.[5] In this case the rotor tested was double the solidity of the Sikorsky R-4B blades, and the air force coefficients have accordingly been halved.

The available data on the pitching moment of the fuselage was very poor. The derivatives of the fuselage were based on the following assumptions

$$C_{D,f} = 0{\cdot}0173,$$

$$C_{m,f} = (-0{\cdot}572 + 2{\cdot}14i)\ 10^{-3}.$$

In evaluating the derivatives, the conditions given in Figs. 1 and 2 for the appropriate airspeeds were used. Other relationships obtained from the flight observations were—

(a) cyclical pitch against airspeed as taken from the curves of Ref. 1 for the appropriate centre of gravity position,

(b) angle of tilt against airspeed as given in Ref. 2,

(c) rotor disc incidence from (b) and the angle of descent (deduced from Figs. 1 and 2).

The following table gives the numerical values of the derivatives used in the stability calculations. The contributions of the fuselage to these derivatives are shown in brackets. As there was no method of allowing for slipstream effects on the fuselage, the fuselage contributions to the total derivatives in autorotation are the same as given for the helicopter flight.

	Helicopter Flight			Autorotation		
	Hovering	30 m.p.h.	60 m.p.h.	Vertical Descent	30 m.p.h.	60 m.p.h.
X_u lb/ft/sec	− 2·02	− 3·8 (−2·0)	− 6·2 (−4·0)		− 19·4	− 15·1
X_w lb/ft/sec	0	− 1·4	+ 0·7	0	− 40·2	− 36·9
X_q lb/radn/sec	+ 99	+174	+183		+176	+ 202
Z_u lb/ft/sec	0	− 16·1	+ 4·15	0	− 68	− 57
Z_w lb/ft/sec		−47·8 (−1·0)	− 65·5 (−2·0)	− 1·2	−242	− 280
Z_q lb/radn/sec		+110	− 21·6		+ 61·6	+ 6·6
M_u ft lb/ft/sec	+10·3	+ 9·9 (−1·4)	+ 8·4 (−2·8)	0	0	0
M_w ft lb/ft/sec	0	+ 14·1 (+2·5)	+ 20·2 (+5·0)	− 6·25	− 77	− 93
M_q ft lb/radn/sec	−512	−910	−945	−840	−825	−1020

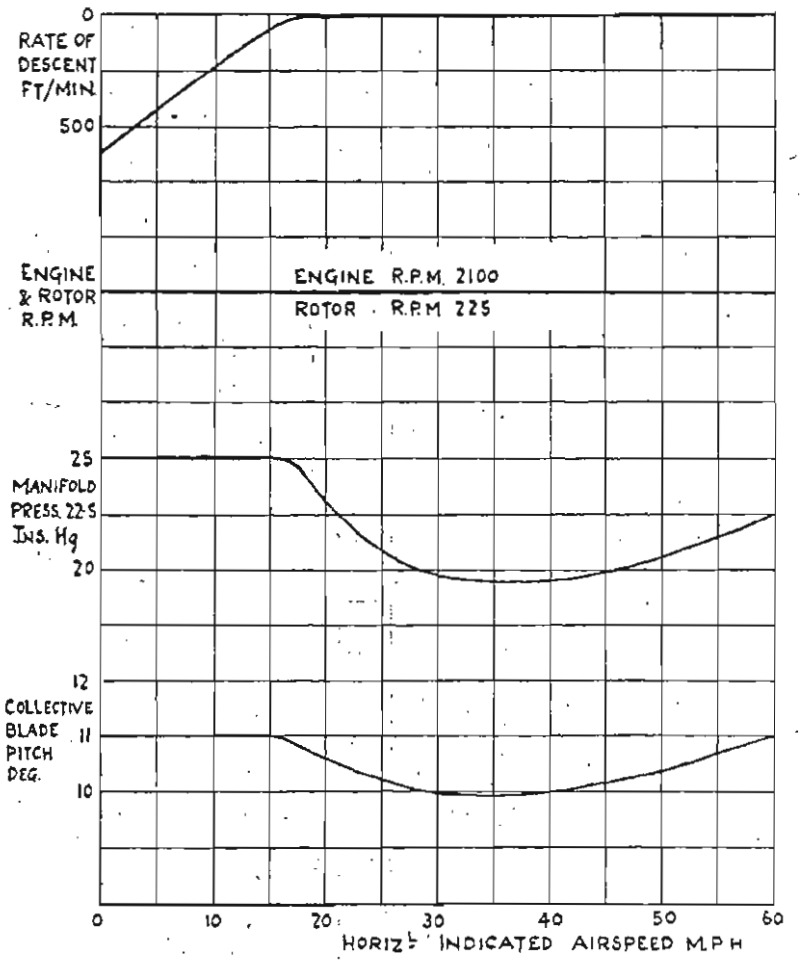

FIG. 1. Initial flight conditions for the phugoid tests—power on.

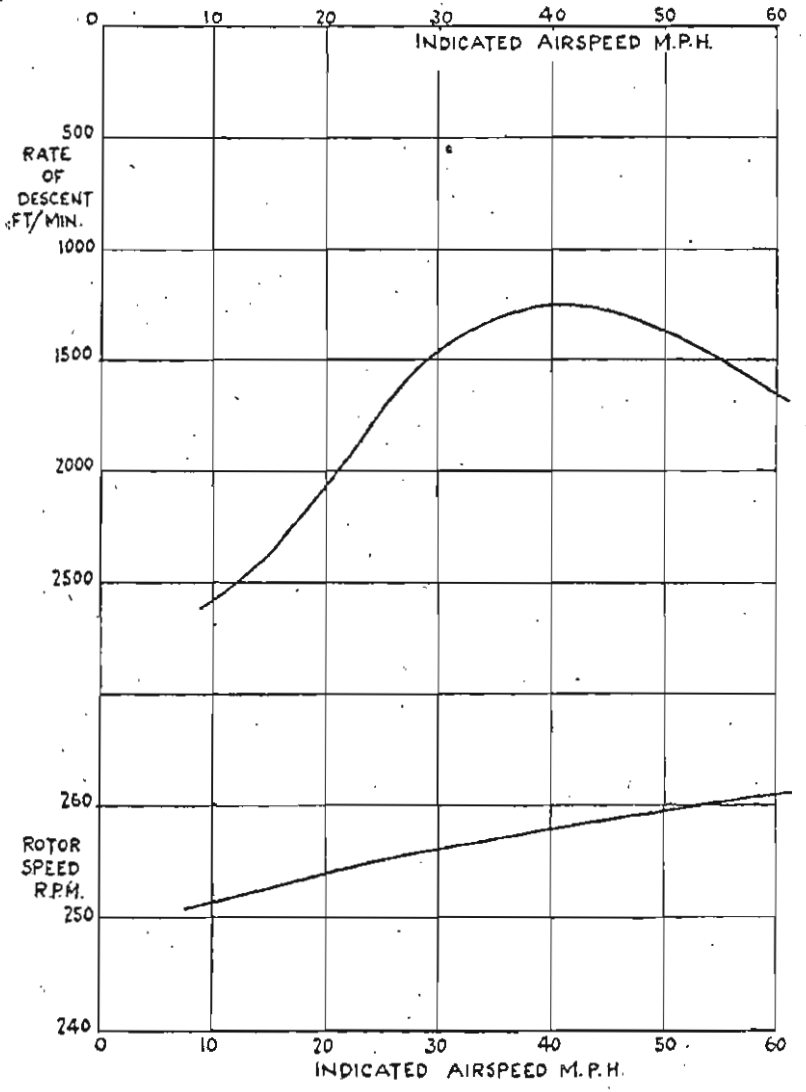

FIG. 2. Initial flight conditions for the phugoid tests—autorotation. $2\frac{1}{2}$ deg collective pitch.

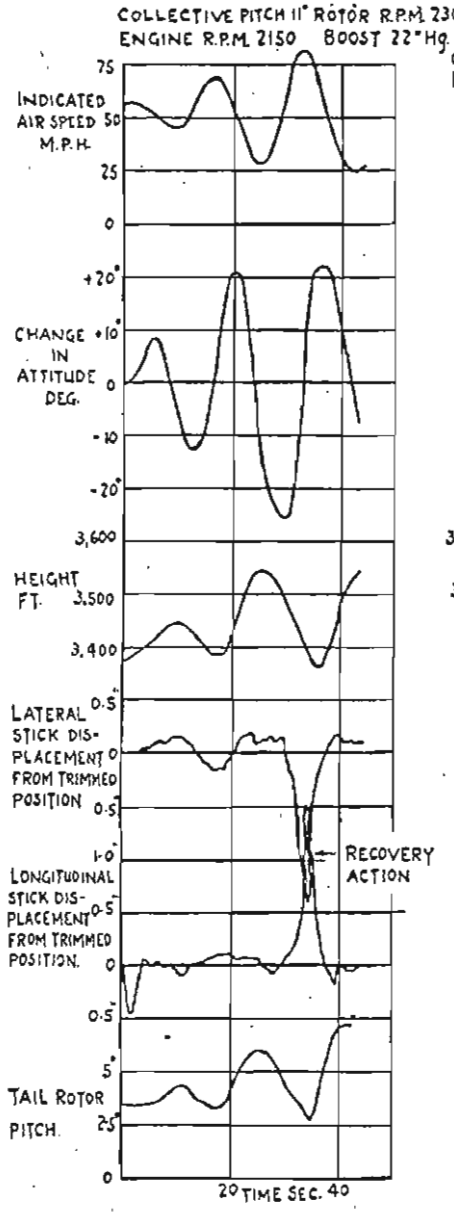

FIG. 3.

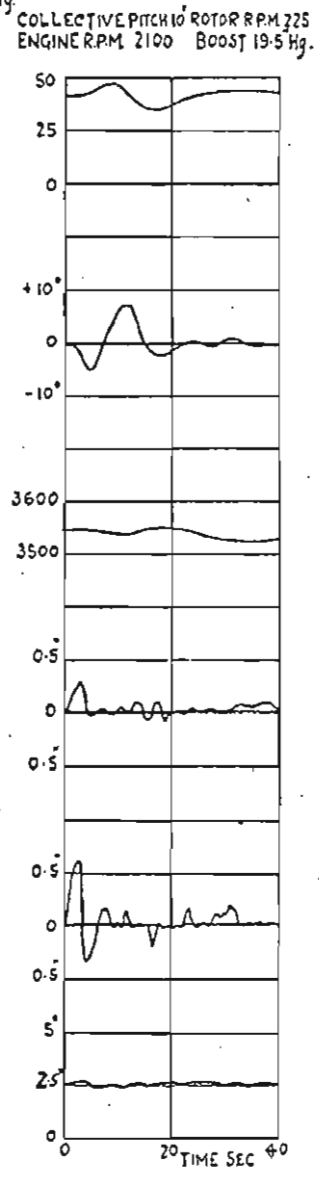

FIG. 4.

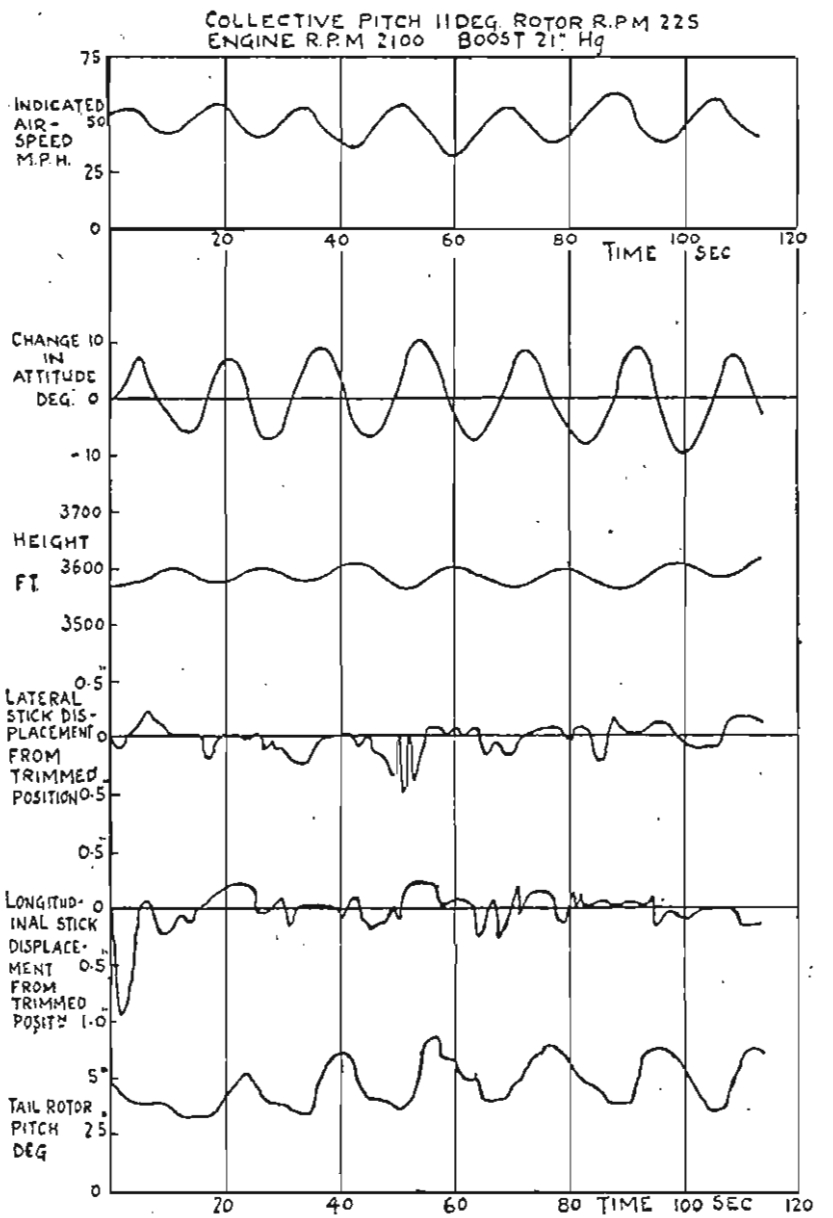

FIG. 5.

Typical records of longitudinal motion from level flight.

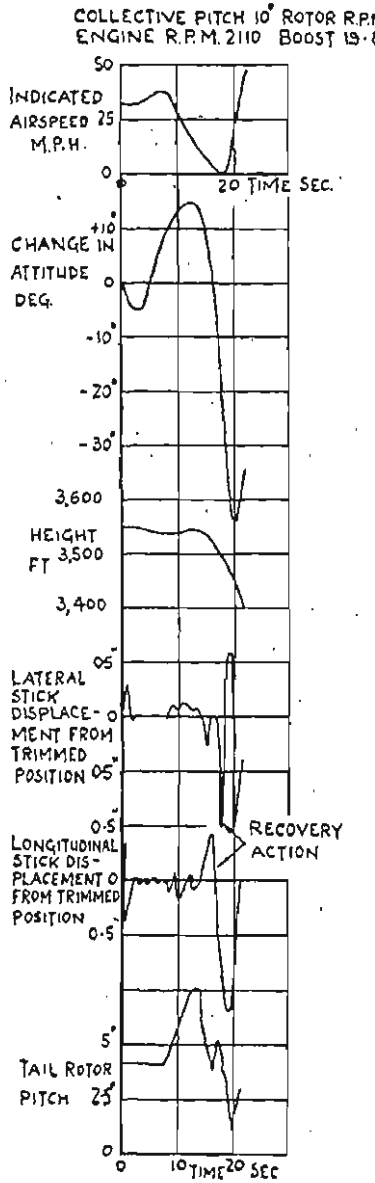

FIG. 6.

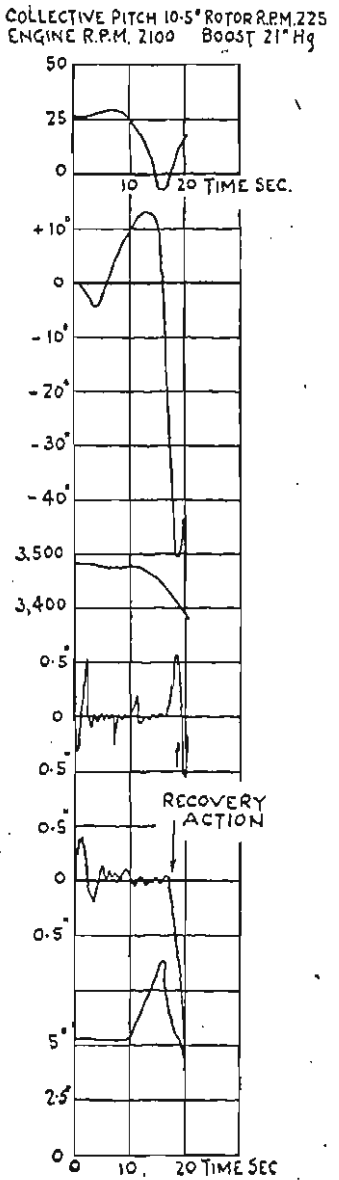

FIG. 7.

Typical records of longitudinal motion from level flight.

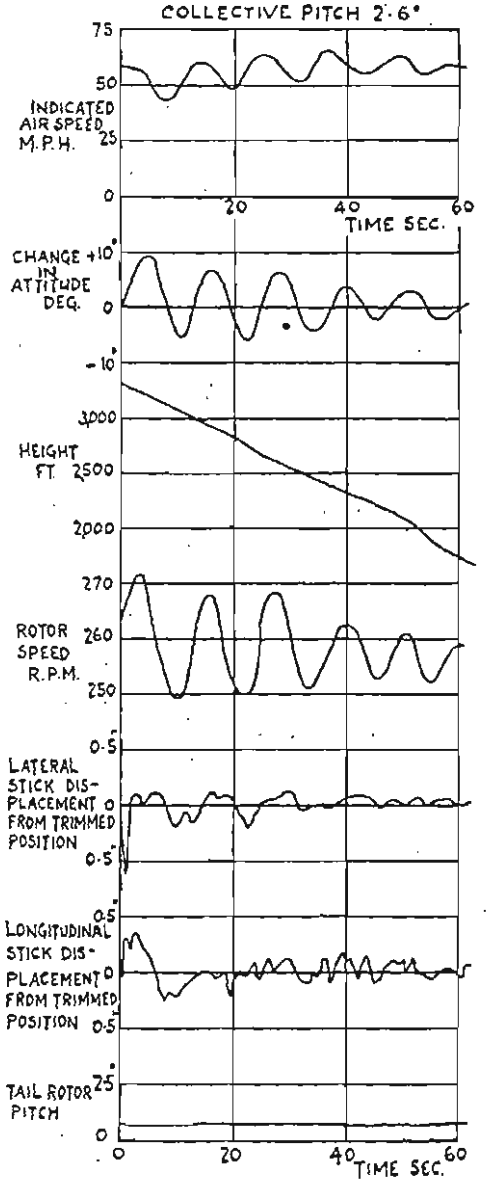

FIG. 8.

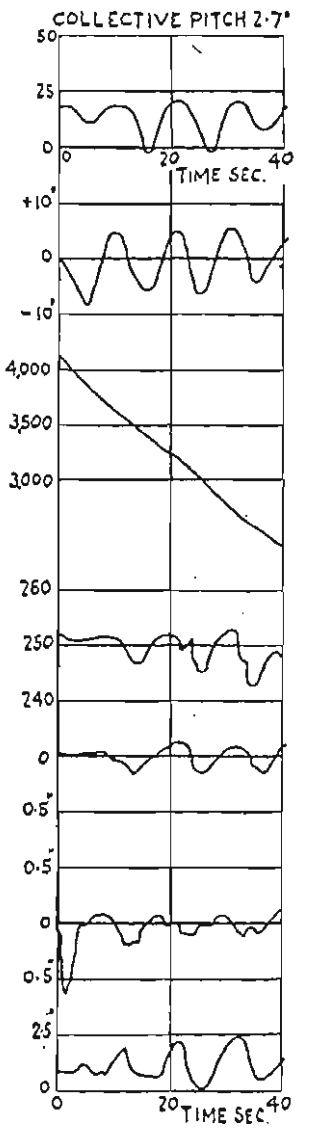

FIG. 9.

Typical records of longitudinal motion in autorotation.

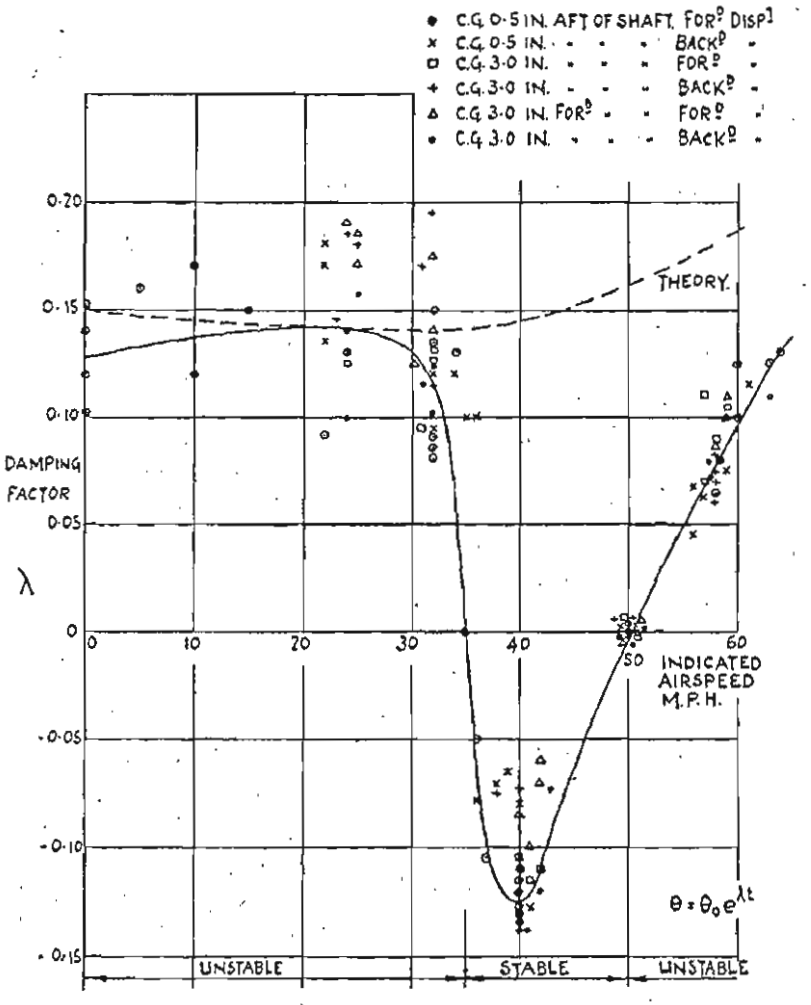

FIG. 10. Damping factor λ.—Power-on conditions.

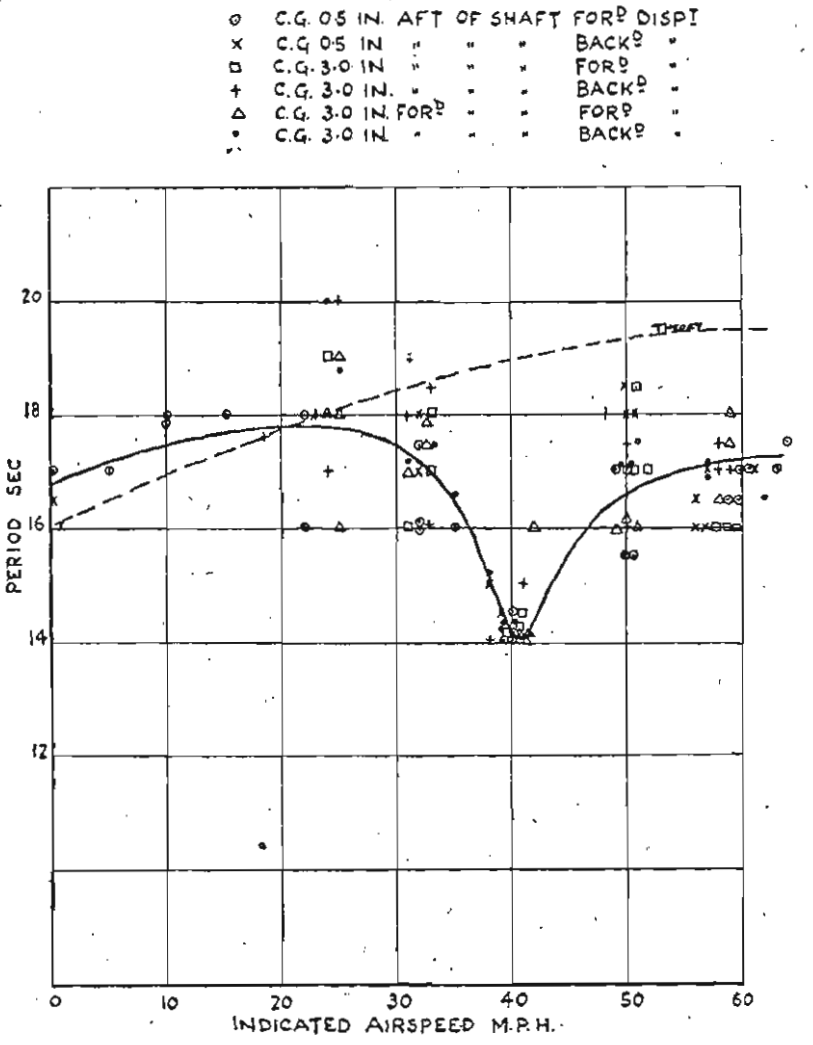

FIG. 11. Periodic time of oscillation.—Power-on conditions.

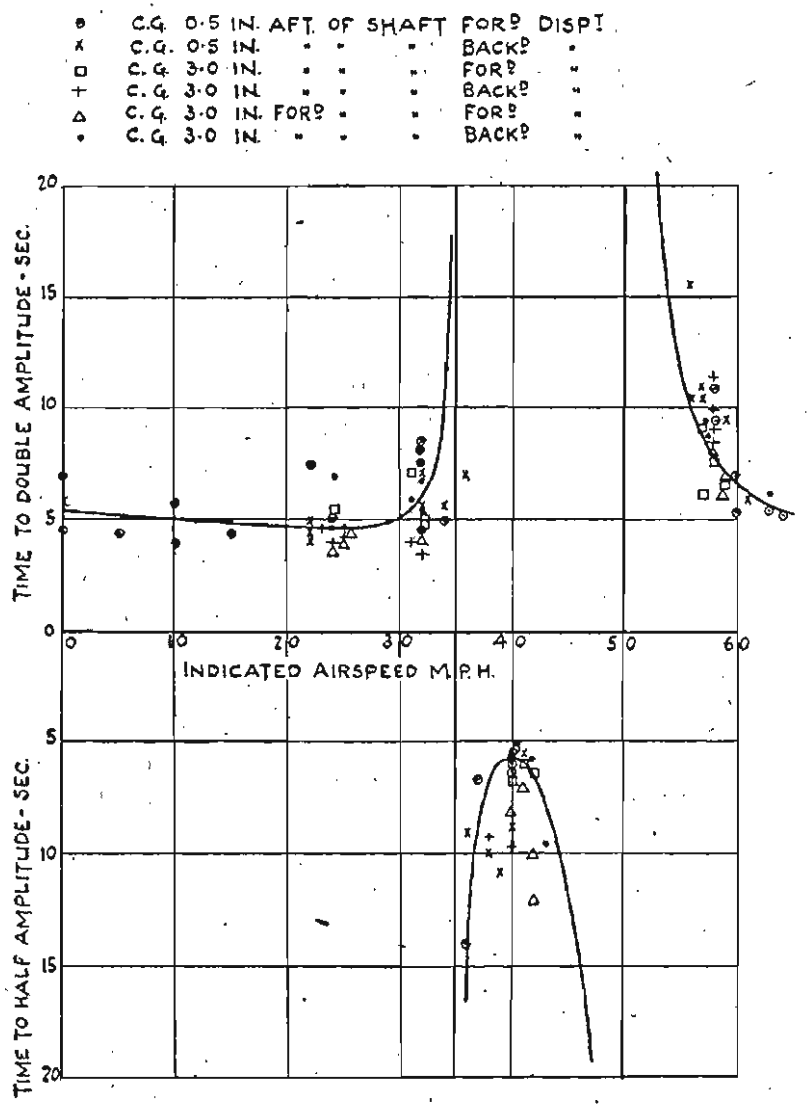

FIG. 12. Time to double or halve amplitude.—Power-on conditions.

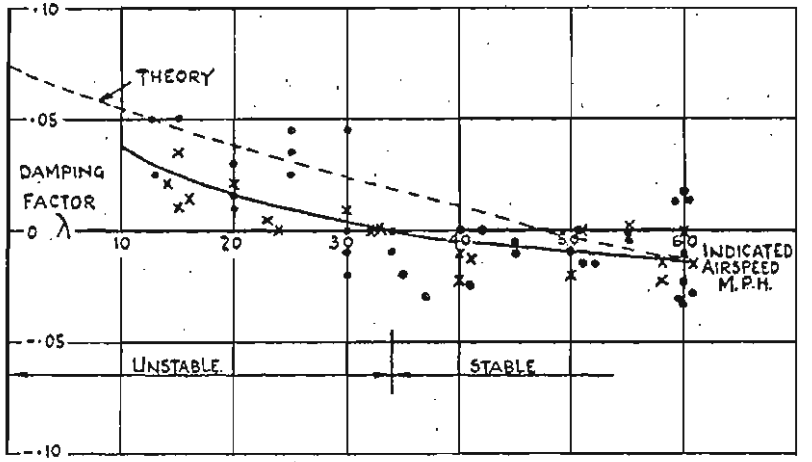

FIG. 13. Damping factor λ.

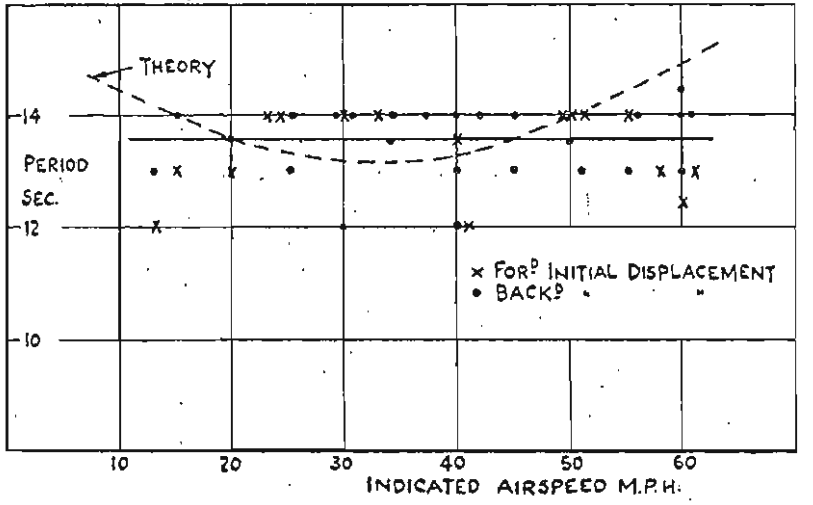

FIG. 14. Periodic time of oscillation.

Dynamic stability tests in autorotation.

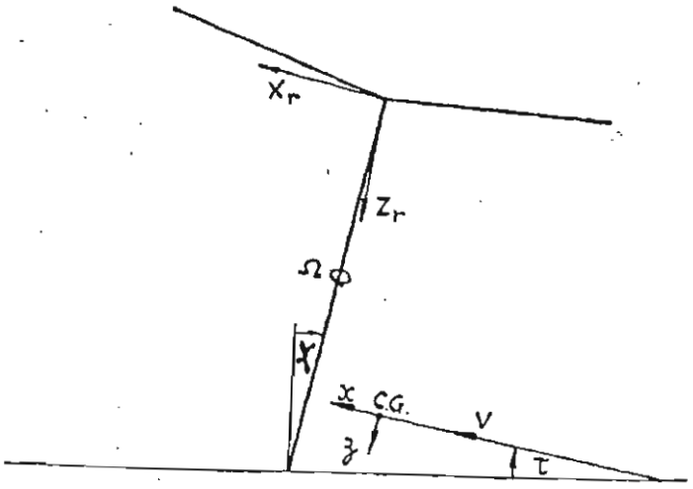

FIG. 15. Nomenclature diagram.

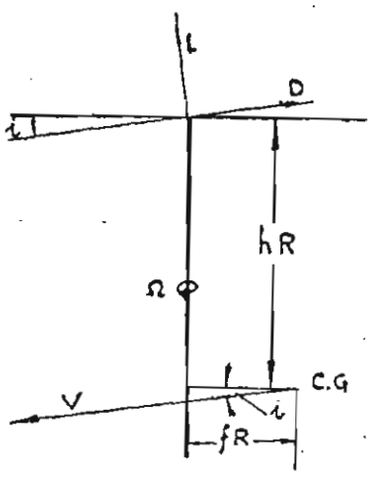

FIG. 16. Nomenclature diagram.

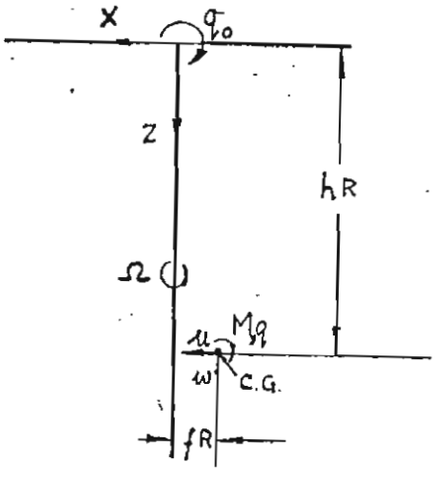

FIG. 17. Hovering flight.

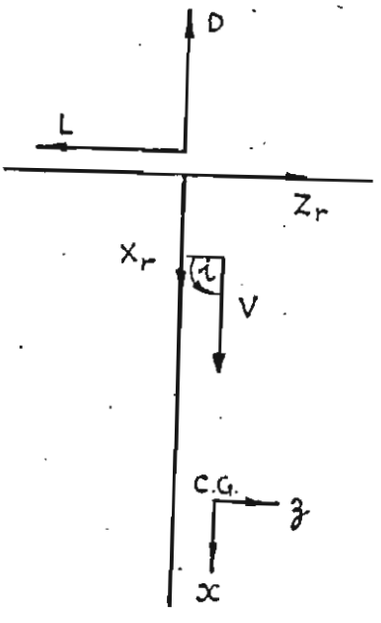

FIG. 18. Vertical descent.

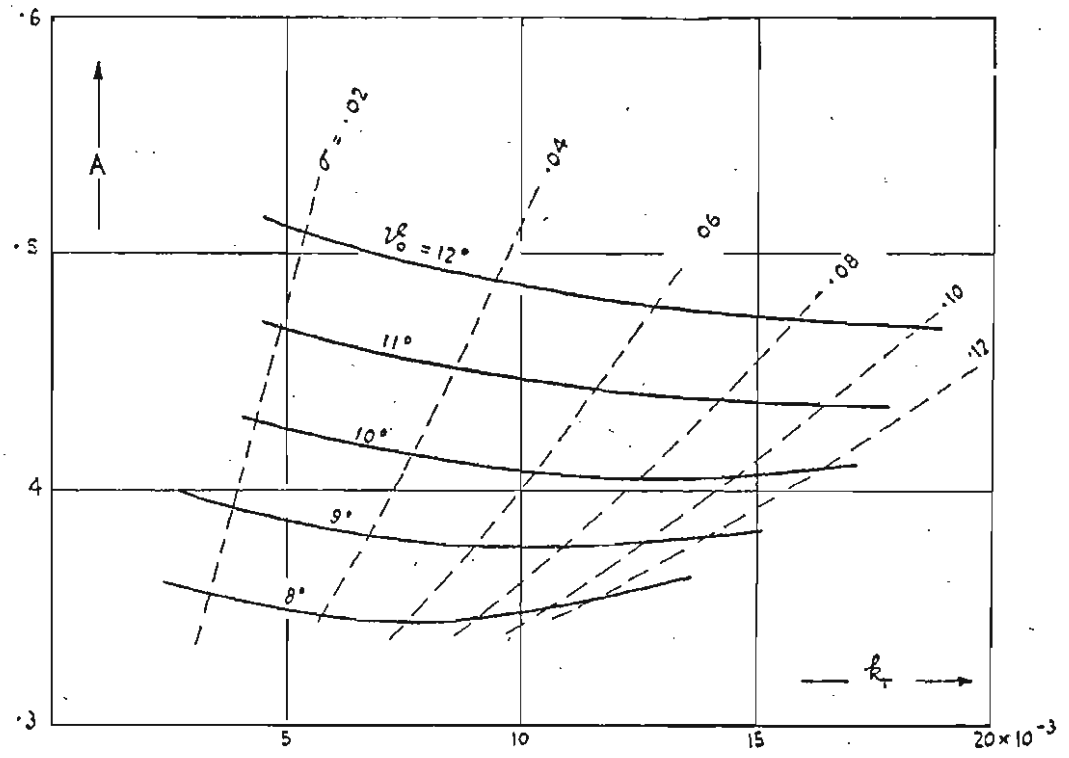

FIG. 19. Chart for coefficient A.

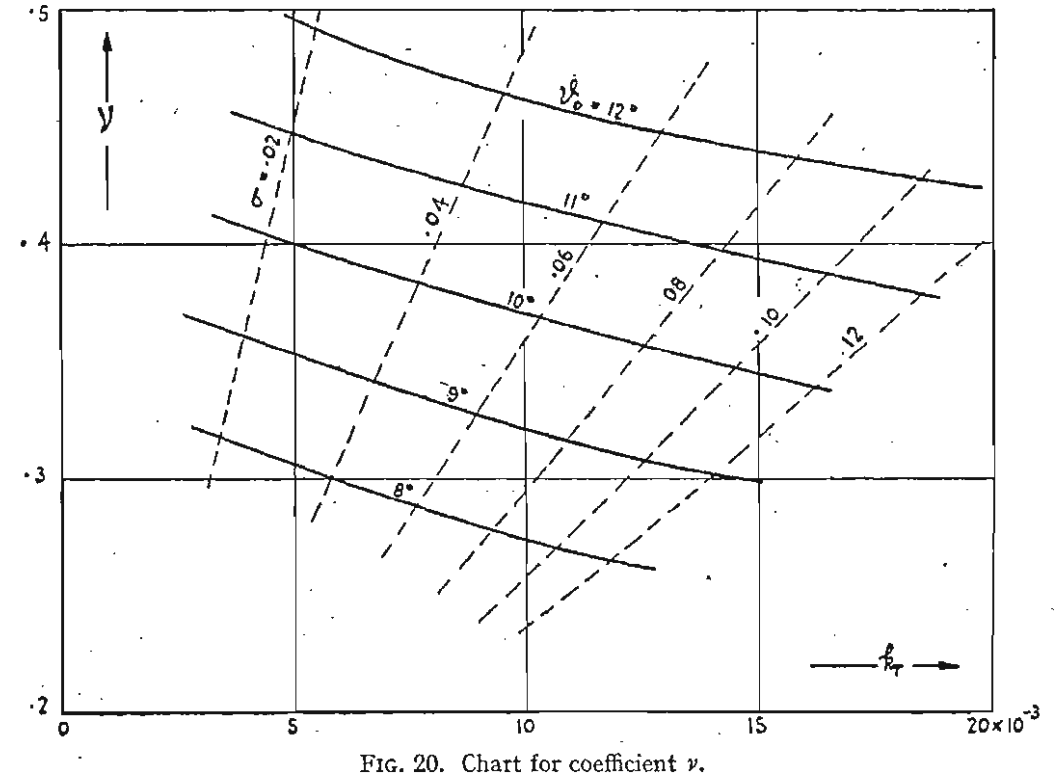

FIG. 20. Chart for coefficient ν.

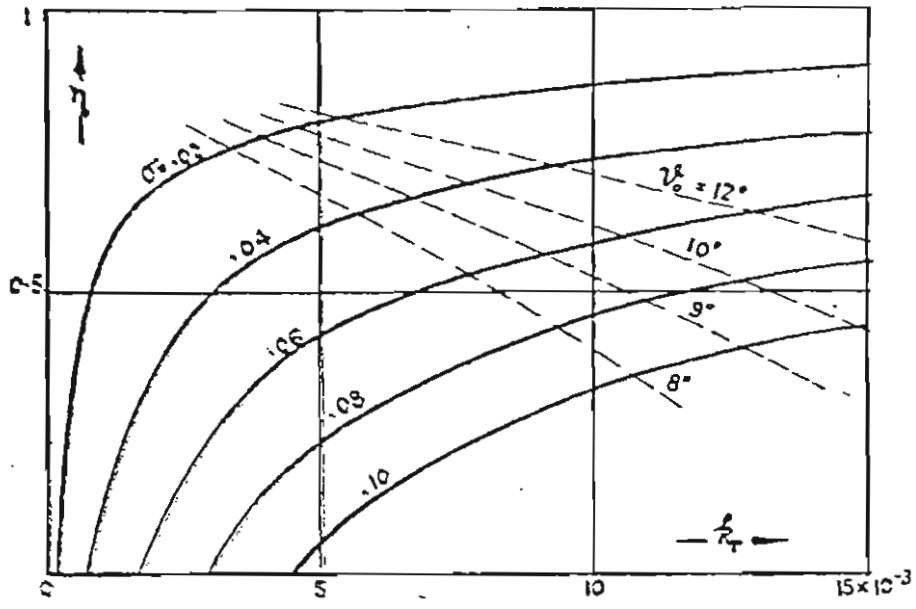

FIG. 21. Chart for coefficient η_1.

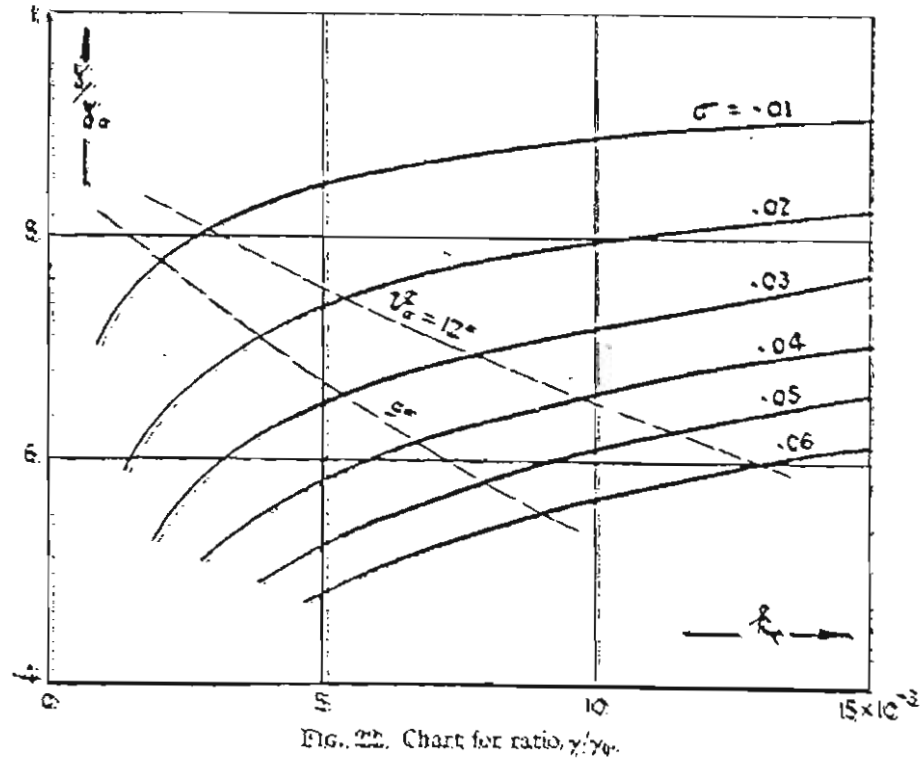

FIG. 22. Chart for ratio γ/γ_0.

Wt. 17-K29. 4/57 G.G.

PRINTED IN GREAT BRITAIN